Experimental Verification of the Hybrid Smart Antenna Algorithm With Modulated Waveforms

Nuri Celik, *Student Member, IEEE*, Magdy F. Iskander, *Fellow, IEEE*, and Zhijun Zhang, *Senior Member, IEEE*

***Abstract*—The hybrid smart antenna approach utilizes a subset of array elements selected according to the receive signal strengths to perform beamforming, thus improving the computational efficiency, and reducing the hardware implementation cost. The previous implementations and published experimental results of this algorithm have been based on continuous-wave (CW) transmit signals, and without modulation. In order to verify the operation of the hybrid smart antenna algorithm with modulated waveforms, the developed 2.4- and 60-GHz testbeds are modified to generate and receive data modulated waveforms. The modifications also include the use of preamble bits at the beginning of each data frame transmitted, and implementation of a sliding window correlator at the receiver to synchronize with the data frames. Binary phase shift keying (BPSK) modulation is used with a 1 megabit per second (Mb/s) data rate for information transfer. The obtained beam patterns agree well with the theoretical results thus verifying the developed hybrid smart antenna algorithm.**

***Index Terms*—60 GHz, adaptive smart-antennas, beamforming, hybrid smart-antennas, low-cost antenna array, modulation, wireless communications.**

I. Introduction

SMART antenna systems utilize multiple antennas and adaptively steer their beam patterns to increase the antenna gain, and reduce multipath fading [1], [2]. Moreover, depending on the number of elements on the array, several nulls in the beam pattern can be formed corresponding to the interferer locations. These features of the smart antenna systems, consequently increase system capacity, extend communication range, and reduce bit error rates.

Although the performance of the smart antenna systems increase by the number of elements on the array, additional costs arising due to the RF hardware requirements, and computational complexity limit the possible number of elements. For instance, the computational requirements of the adaptive weight calculation algorithm increase exponentially with the number of array elements, thus, driving the computational time of the system up (ON^2 for the very popular least mean squares algorithm where N is the number of array elements), and increasing the tracking delay [1]. To avoid these limitations and high costs, antenna switching is proposed in the literature as an alternative [1]. Antenna switching employs several directional antennas and selects the antenna with the highest received signal power. This system has very low computational complexity, and relatively low hardware cost, however it suffers from scalloping effects and its angular resolution is limited.

Taking into account these advantages and limitations, our group proposed a hybrid smart antenna system that combines the advantages of the adaptive smart antenna and the antenna switching approaches [3]. This system employs an array of directional elements arranged in a linear geometry but each tilted at a different angle with respect to the array axis. The tilt angles are optimized to yield the best performance with minimal scalloping effects [4]. The algorithm selects the subset of the array elements with the highest total receive signal power for the beamforming stage significantly reducing the computational complexity. The performance of the proposed hybrid smart antenna system was evaluated by computer simulations in [5] and experimentally in [6], [7], and [8]. In [8], it was also shown that for a 60-GHz system, the cost savings due to use of a hybrid smart antenna system is very significant because of very high RF component prices.

All the previously mentioned experimental verification of the hybrid smart antenna algorithm have been conducted using a continuous–wave (CW) signal at the transmitter, thus, eliminating the need for Tx-Rx synchronization. For upgrading the existing 2.4- and 60-GHz testbeds to handle modulated waveforms, however, a wireless synchronization mechanism has to be implemented. This letter briefly describes some of these modifications and presents the obtained experimental results both at 2.4 and 60 GHz.

The rest of the letter is organized as follows. In Section II, the adaptive weight update operation is briefly described. Section III describes the required modifications in the testbeds and their implementation. Section IV contains the experimental results and discussion of the obtained results. Section V concludes the letter.

II. Problem Formulation

In this section, the weight update operation is briefly described, a detailed version is included in [7]. The transmitted signal $d(t)$ coming from the direction (θ', ϕ'), impinges upon the antenna array, and it is assumed to be narrowband such that its complex envelope does not change through the array. This assumption requires that the total length of the array L should satisfy the following relation:

$$L \ll cT_s \tag{1}$$

where c is the speed of light and T_s is the symbol period.

If the received signal vector at the array is $\mathbf{u}(t)$, the output of the beamformer is

$$\hat{d}(t) = \mathbf{w}^H(t)\,\mathbf{u}(t) \tag{2}$$

Manuscript received November 11, 2008; revised January 16, 2009. First published February 02, 2009; current version published May 06, 2009.

N. Celik and M. F. Iskander are with the Hawaii Center for Advanced Communications, University of Hawaii at Manoa, Honolulu, HI 96822 USA (e-mail: celik@hawaii.edu; iskander@spectra.eng.hawaii.edu).

Z. Zhang is with the Department of Electronic Engineering, Tsinghua University, Beijing 100084, China (e-mail: zjzh@tsinghua.edu.cn).

Digital Object Identifier 10.1109/LAWP.2009.2014401

where $\mathbf{w}$ is the complex vector of beamforming weights, and subscript H stands for the Hermitian of the vector. The LMS algorithm updates these weights as follows:

$$\mathbf{w}(t+\Delta t) = \mathbf{w}(t) + \mu e^{*}(t)\,\mathbf{u}(t) \tag{3}$$

$$e(t) = d(t) - \hat{d}(t). \tag{4}$$

As seen in (3), the weights are updated according to the error between the system output and the desired signal and μ adjusts the magnitude of the updates. The superscript $*$ denotes the complex conjugate operation. The maximum value of μ determined by the eigenvalues of the received signal's autocorrelation matrix must not be exceeded in order to ensure convergence.

III. Modifications and Implementation

As indicated in (4), the transmitted signal should be known at the receiver to initiate the weight update operation. For this purpose, the data is divided into 450 bit frames and a 50-bit preamble is added in front of each data frame. If the preamble is known at the receiver, the weight update can be possible during preamble transmissions. However, for this to happen, the receiver has to know the timing of the frames precisely so that it can enable the weight update operation requiring a synchronization mechanism.

In digital wireless receivers, the time recovery is usually established through the use of orthogonal waveforms [9]. An orthogonal waveform has a very high correlation with itself but negligible correlation with its time-shifted versions. As a result, timing of the orthogonal waveform can be fully recovered by employing a sliding correlator and detecting the peaks [9] and the accuracy depends on the correlation properties of the selected waveform. In [10], the authors studied and optimized bit-sequences of varying length in terms of their correlation properties. In this letter, the 50-bit preamble sequence "39911AE92BC3E" in hexadecimal format from [10] is selected as the preamble and tested to have good correlation properties. The rest of the frames are filled with random data bits. An Agilent E4438C vector signal generator programmed for the designed frame format with the selected preamble is used to generate the transmit waveform [11]. BPSK modulation with 1-Mb/s data rate is employed at the transmitter, and a root raised cosine filter with 0.35 roll-off factor is used as the pulse shaping filter [9].

As aforementioned, the weight update operation in (3) is designed to minimize the mean square error between the locally generated replica of the preamble waveform and the received preamble waveform. Therefore, large weight updates are expected to occur when the locally generated replica of the preamble is very different from the one that is received. These discrepancies when large can even prevent the algorithm from converging to the correct weights. These differences can stem from the nonlinearities in the RF hardware, bandwidth limitations of the RF devices, and even the differences in the pulse shaping filter coefficients. In order to demonstrate the performance degradation due to nonlinearities in the system, a simple clipping example is simulated. Clipping can be defined as the waveform distortion that occurs when the amplifiers are overdriven above their maximum power capabilities. A k percent clipping operation for a signal $d(t)$ can be mathematically defined as

$$\begin{aligned} \frac{\max(d(t)) \times (1-k)}{100\ if\ d(t)} &\geq \frac{\max(d(t)) \times (1-k)}{100} \\ d_c(t) &= \frac{\min(d(t)) \times (1-k)}{100\ if\ d(t)} \\ &\leq \frac{\min(d(t)) \times (1-k)}{100} \\ &\quad \times d(t)\ \text{otherwise.} \end{aligned} \tag{5}$$

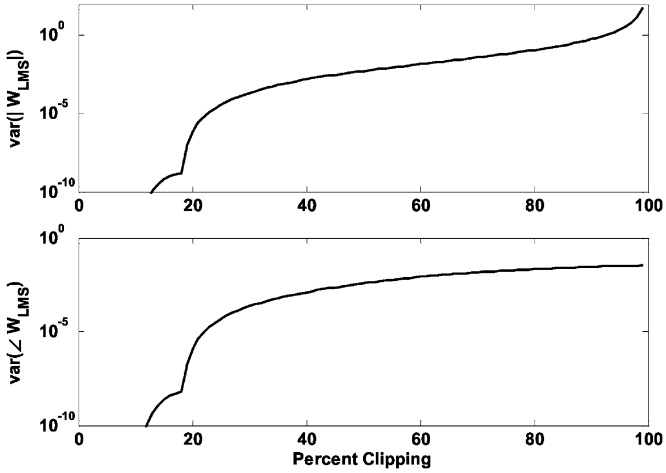

Fig. 1. Change in the variance of the LMS weights due to the increase in the waveform clipping. Top: Magnitude variation. Bottom: Phase variation.

In Fig. 1, the variance of the LMS weights is plotted in terms of magnitude (top), and in terms of phase (bottom). As expected, the algorithm fails to converge to the correct weights with increased clipping as demonstrated by the high variance. The transmitted signal is BPSK modulated with 1 Mb/sec data rate, and the two receive antennas receive exactly the same signal, there is no noise in the system so the weights are expected to converge to the same value of 0.5 and remain constant. However, with above 50% clipping, the variance of the magnitudes of weights becomes equal and larger than the variance of a random variable uniformly distributed between the interval $[0 \quad 0.5]$. Therefore, caution must be exercised in designing the system, to minimize the nonlinear effects.

At the receiver, the correlation is continuously calculated and the data bits corresponding to preamble are used as the desired signal for the weight update whenever a correlation peak is found. To eliminate the synchronization errors due to the phase discrepancy between the Tx and Rx oscillators, a quadrature demodulator is employed.

IV. Experimental Results

In this section, the results of the 2.4- and 60-GHz testbeds will be presented, details of implementation and the calibration procedures are described in previous publications [6]–[8].

A. 2.4-GHz Testbed Results

As there is significant multipath and noise in this frequency bands, the experiments are conducted inside an anechoic chamber in order to obtain meaningful beam patterns. The computer handling the A/D conversion and beamforming

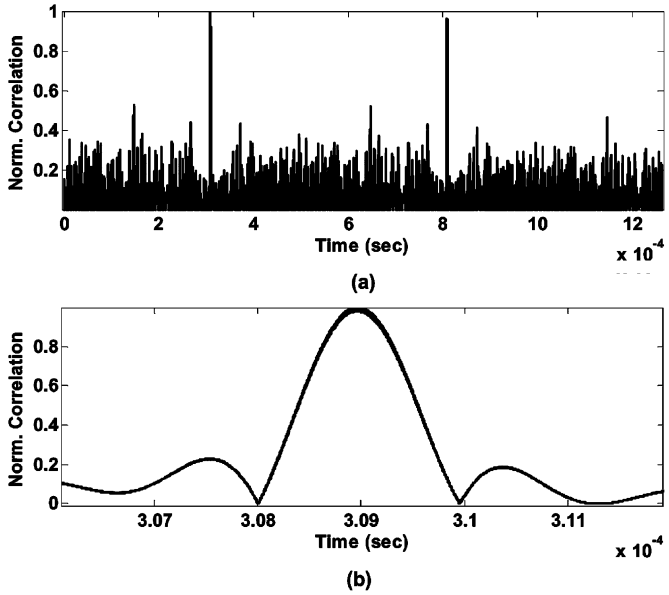

Fig. 2. (a) Correlation versus time. (b) Magnified plot of correlation at the start of the first frame.

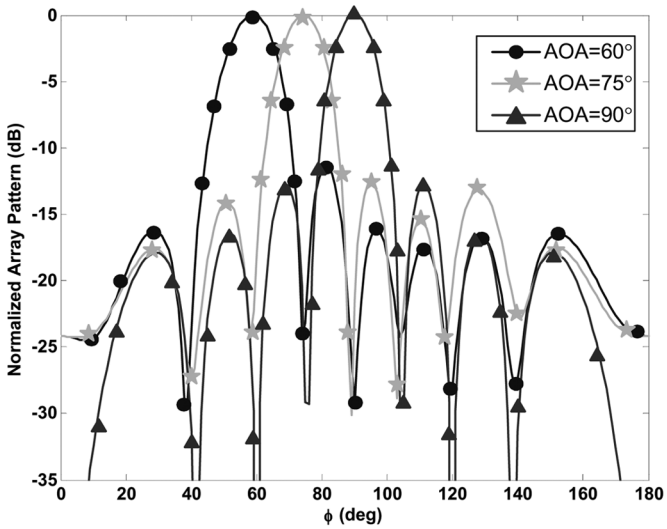

Fig. 3. Beam patterns when $\mathrm{AOA} = 60°$, $\mathrm{AOA} = 75°$, and $\mathrm{AOA} = 90°$.

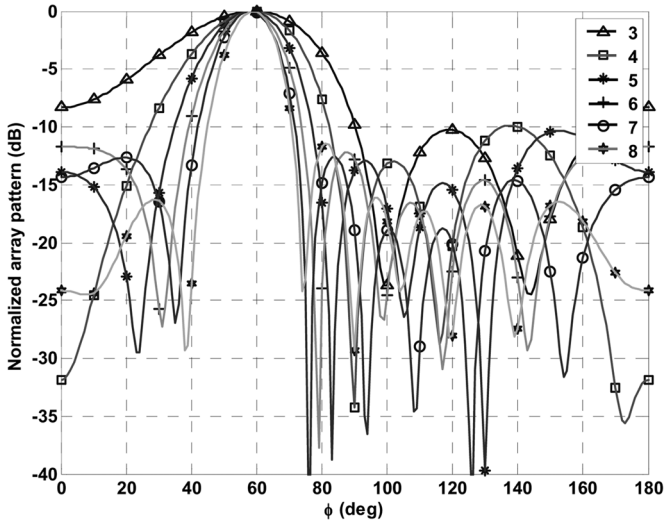

Fig. 4. Beam patterns when $\mathrm{AOA} = 60°$ for different number of array elements selected.

operations is controlled from outside the chamber by a remote desktop connection. A BSPK modulated signal with 2.4-GHz center frequency and 1-Mbps data rate is transmitted by a horn antenna and the receiving array has 8 isotropic (sleeve antenna) elements. The smart-antenna testbed downconverts the carrier frequency to 5 MHz and then digitizes at 25 MSample/s by an 8-channel analog-to-digital converter (ADC). In all of the experiments, the elevation angle θ' is selected to be $\pi/2$ and the azimuth angle ϕ' corresponding to the angle of arrival (AOA) of the signal is calculated from the obtained combining weights and compared to the actual AOA. The received bandpass signal is converted to its low-pass equivalent by calculating its Hilbert transform. Sliding window correlation operation is applied to all the received signals and the most repeated peak position is selected as the synchronization point to prevent errors due to failure of receiver channels. As shown in Fig. 2, the correlation peak locations coincide for all eight channels pointing out perfect synchronization for all the receiver channels.

After ensuring that the synchronization mechanism works, the calibration procedure described in [7] is completed and the LMS weight vectors for several AOA are obtained. The beam patterns corresponding to these weight vectors are then calculated assuming isotropic radiation patterns. In order to ensure that the sampling rate is sufficiently high to prevent sampling phase errors, the received data is interpolated by 10. In this case the LMS errors for all angle of arrivals turn out to be on the order of 10^{-5}, indicating a good convergence of the weights.

In order to check if the system works as expected, the system is first configured as a typical smart antenna system using all the eight receiver channels. In Fig. 3, the beam patterns corresponding to $\mathrm{AOA} = 60°$, $\mathrm{AOA} = 75°$, and $\mathrm{AOA} = 90°$ cases are plotted, and it is seen that the system is able to accurately steer its receive beam in the signal direction.

As aforementioned, hybrid beamforming algorithm reduces the complexity of the beamforming operation by selecting a subset of the elements on the array. The beam pattern corresponding to different number of selected array elements is shown in Fig. 4 for $\mathrm{AOA} = 60°$. As expected, slightly higher sidelobes and wider main lobes are observed as the number of selected elements is reduced, thus, agreeing with the previous results obtained using CW signals [6]–[8]. The proposed hybrid smart antenna system was, thus, able to determine the correct AOA for modulated signal even with only three antennas selected and the maximum sidelobe level does not exceed -10 dB.

B. 60–GHz Testbed Results

The test procedure applied here is very similar to the one explained in [8]. Agilent E4438C signal generator is set to generate a BPSK signal with 1-GHz center frequency and this signal is mixed with a 59-GHz sine wave to obtain the 60-GHz modulated signal. The transmit horn antenna is located 50 cm from the receiver, and the receive horn antennas are spaced 5.1 cm apart. To establish significant beam overlapping, one of the antennas is tilted 12° with respect to the array axis, so that its radiation pattern peak points to 78° as opposed to 90° as shown in Fig. 5.

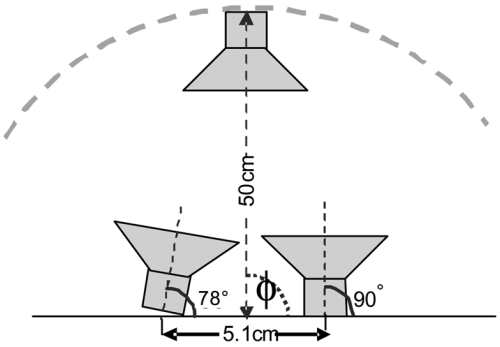

Fig. 5. Measurement setup for the 60-GHz experiments. Please note that the peaks of the element radiation patterns are directed to different angles (78° versus 90°) to ensure significant radiation pattern overlap.

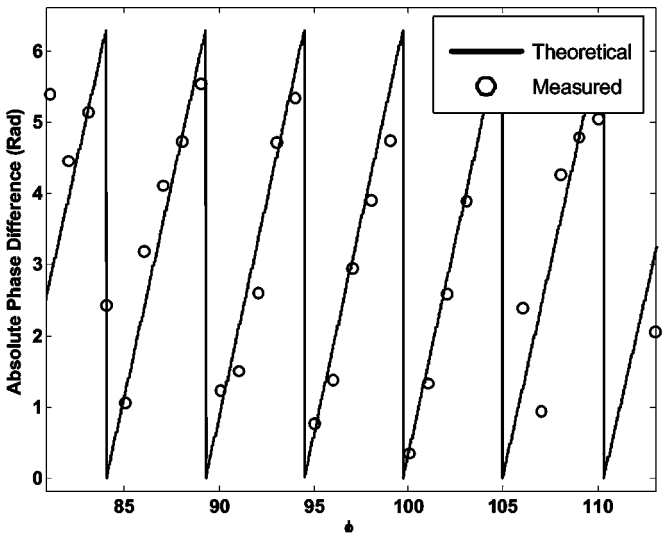

Fig. 6. Theoretical and measured phase differences.

The signal format and the synchronization mechanism are the same as the 2.4 GHz case, only difference being the bandpass filter centered around 5 MHz to eliminate the harmonics due to nonideal characteristics of the 60-GHz mixers.

For verifying the correct operation of the system, the estimated phase differences between the signals and the theoretical phase difference is calculated and plotted in Fig. 6. Due to large spacing of the array elements compared to the wavelength, and weak signal levels resulting from narrow antenna beamwidths, the phase difference changes rapidly and one can observe large deviations with the increase of scan angle from the calibration center, 95°. Fig. 7 demonstrates the resulting beam pattern for various AOA, for which the system was able to steer the beam peak to the desired location. The other two peaks in each of the radiation patterns are due to large spacing of the array elements and are called the grating lobes [1]. For the angular range of 93° to 97°, the beam peak is indeed at the transmitter direction, and its normalized power is larger than the grating lobes.

V. Conclusion

In this letter, the experimental results of two smart-antenna testbeds employing the hybrid beamforming algorithm proposed in [3] are presented. The preamble added to the transmitted data frames is used to establish synchronization, as well as to help the receiver generate a local replica of the transmitted signal for weight calculation operation.

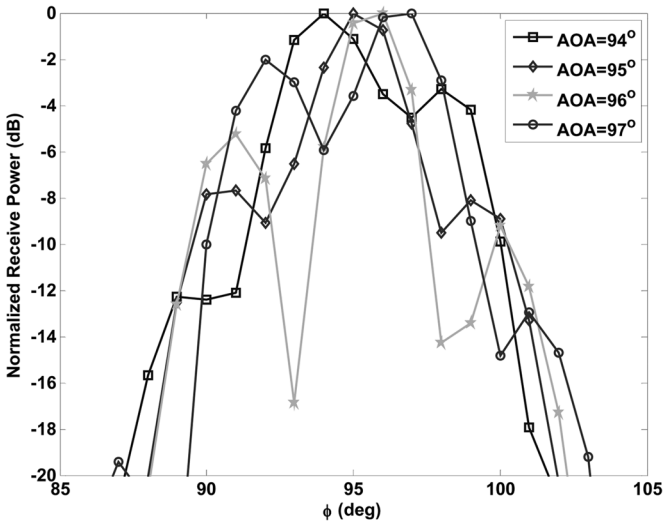

Fig. 7. Beam patterns for various AOA.

The results obtained using modulated data are consistent with simulation results given in [5] and experimental results given in [6]–[8] and suggest that a hybrid beamforming algorithm is a promising method for decreasing hardware related costs, as well as computational complexity and thus resulting in a higher tracking speed. The experimental results show in all cases that, the smart-antenna prototypes are able to determine the correct angle of arrival and steer the beam to the transmitter direction.

References

[1] J. C. Liberti and T. S. Rappaport, *Smart Antennas for Wireless Communications: IS-95 and Third Generation CDMA Applications*. Englewood Cliffs, NJ: Prentice–Hall, 1999.

[2] L. C. Godara, "Applications of antenna arrays to mobile communications, part II: Beam-forming and direction-of-arrival considerations," *Proc. IEEE*, vol. 85, pp. 1195–1245, Aug. 1997.

[3] Z. Zhang, M. F. Iskander, Z. Yun, and A. Host-Madsen, "Hybrid smart antenna system using directional elements—performance analysis in flat Rayleigh fading," *IEEE Trans. Antennas Propag.*, vol. 51, no. 10, pp. 2926–2935, Oct. 2003.

[4] N. Celik and M. F. Iskander, "Genetic algorithm based antenna array design for a 60 GHz hybrid smart antenna system," *IEEE Antennas Wireless Propag. Lett.*, vol. 7, pp. 795–798, 2008.

[5] M. Rezk, W. Kim, Z. Yun, and M. F. Iskander, "Performance comparison of a novel hybrid smart antenna system versus the fully adaptive and switched beam antenna arrays," *IEEE Antennas Wireless Propag. Lett.*, vol. 4, pp. 285–288, 2005.

[6] N. Celik *et al.*, "Implementation and experimental verification of hybrid smart-antenna beamforming algorithm," *IEEE Antennas Wireless Propag. Lett.*, vol. 5, pp. 280–283, 2006.

[7] M. Iskander *et al.*, "Antenna arrays technologies for advanced wireless systems," in *Modern Antenna Handbook*, C. A. Balanis, Ed. New York: Wiley, 2008.

[8] N. Celik *et al.*, "Implementation and experimental verification of a smart antenna system operating at 60 GHz band," *IEEE Trans. Antennas Propag.*, vol. 56, pp. 2790–2800, Sep. 2008.

[9] J. G. Proakis, *Digital Communications*. New York: McGraw-Hill, 1995.

[10] A. Atalar and S. E. Kocabas, "Binary sequences with low aperiodic autocorrelation for synchronization purposes," *IEEE Commun. Lett.*, vol. 7, no. 1, pp. 36–38, Jan. 2003.

[11] *Agilent Technologies, Agilent E4438C Vector Signal Generator User Guide*. Santa Clara, CA: Agilent Technologies Inc., 2007.